An Analytical Model for Detailed Transient Fault Analysis of Doubly-Fed Induction Machines

Frederic Maurer and Jonas Kristiansen Nøland

***Abstract*—This paper presents an exact analytical solution to the two-phase and three-phase short-circuit events of the doubly-fed induction machine (DFIM). The contribution is intended to strengthen the predictability of DFIMs under the design stage or for control tuning purposes and reduce the computational costs of large-scale transient stability studies of the interconnected power system. In general, the approach enables to simplify and improve the analysis DFIMs. The original analytical equations are derived from first principles. A case study of a doubly-fed induction generator (DFIG) is considered, where the "large machine approximation" is shown to be valid as well. The analytical equations are used to predict the torque transients in different handpicked transient scenarios and assessed against numerical simulations. Finally, the proposed analytical model shows excellent agreement with the numerical results in the SIMSEN environment.**

***Index Terms*—Analytical modeling, doubly-fed induction generator (DFIG), induction machines, transient stability.**

I. Introduction

The doubly-fed induction machine (DFIM) is applied in a wide variety of power generation facilities. In general, there are issues related to the mechanical design, the control design, as well as to the interplay with the power grid [1], where transients can be induced. The machine current and torque transients are critical machine-related issues, as their maximum values determine the mechanical design. The DFIM must withstand these stresses without any damages, e.g., mechanical vibrations in the winding overhang of large DFIMs. As the rotor frequency can vary in a range of -10%-10% of slip (for hydro-generator applications) and up to a range of -30%-30% of slip (for wind turbine applications), it is very likely that the DFIM will experience vibration even during normal operation. For instance, rotor harmonics [2] or even supply induced harmonics [3] can lead to vibrations. Easy-to-use and simplified analytical equations are needed to give a go/no-go decision for DFIMs. In fact, a detailed analysis that would require huge computational effort (up to several days for the most complex 3D-FE models), namely, FE electro-magnetical and mechanical calculation. So the biggest contribution of this paper is a significant computation time reduction during the electrical design phase of a large size DFIM.

From the grid perspective, the phenomena occurring during a fault-ride through (FRT) event are much more relevant [4]–[8]. In these cases, the grid owner normally requires that the

F. Maurer is with EPFL, Lausanne, Switzerland (email: frederic.maurer@me.com).

J. K. Nøland is with the Department of Electric Power Engineering, Norwegian University of Science and Technology, Trondheim, Norway.

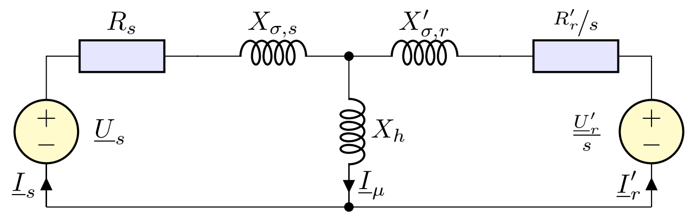

Fig. 1. Equivalent scheme of the DFIG

machine can stay connected to the grid after such a transient phenomenon. The current and torque amplitudes of these phenomena are lower than for a terminal short-circuit fault so, i.e., they do not significantly impact the mechanical design of the generator (local ones are more severe). The grid faults are normally simulated using numerical simulation software like SIMSEN[1], as the grid topology is different for every project.

Recently, simplified models have been proposed for the DFIM under steady-state and transient operations [9], [10]. [11] presented a harmonics analysis of the double output induction generator. The applications of transient models include improvement of the DFIM controllers [12], as well as reducing the computational cost of large-scale transient stability studies [13]. This paper takes the transient domain a step further. A complete set of transient equations of an induction machine is presented in [14], whereas the well-known expression for an induction machine (doubly fed or not) can be found in [15]. The original contribution of this study lies in the transient equation for DFIM applicable for the "large machine assumption" [15], which can be derived using the work done in [14] adapted for a DFIM. The exact analytical equation for predicting the two-phase short-circuit is presented. In addition, the analytical equations provide a piece of frequency information, which is used to ensure that no mechanical eigenmodes can be triggered by a severe transient in the complete operating range of a DFIG.

The remainder of the paper is organized as follows. Section II presents the modelling hypothesis and its analytical model. The transient analytical equations of the DFIG is derived in Section III. Then in Section IV, the equations are validated against a numerical simulation model. Finally, Section V concludes the paper.

[1] http://simsen.epfl.ch

II. Theory framework and Basic assumptions

This section is dedicated to describe the assumptions underneath the short-circuit fault modelling problem of this paper.

A. Modelling Hypothesis

The following assumptions are given, which are common in transient analysis of big electrical machines [15], [16]. The resistances are constant and at a given temperature [15]. The saturation of the main inductance is neglected [15]–[17]. Saturation may exist prior to the faulty condition. These quantities are governed by the saturation of the stator and rotor leakage reactance, which can be integrated by reducing the leakage reactances by 10-20% depending on the initial saturation level of the machine [16]. The machine can be considered in steady-state conditions with constant torque before the short-circuit with constant speed during the short-circuit.

The voltage-sourced inverter (VSI) is modelled with a constant voltage source so that its influence is neglected during the short-circuit [15]. The VSI is assumed to continue to provide the same rotor voltage as before the transient, which is not strictly realistic, as the semi-conductors cannot handle this huge amount of current flowing easily during the transients.

In reality, there is a resistive crowbar going into operation, when the machine and/or the VSI protection decides to fire it [17]. This firing is done to limit the current in the VSI. But it will take from 5-10ms to fire the crowbar, implying that the first and most important current and torque peak will happen without the impact of the crowbar. In the case of the firing of the crowbar, the rotor voltage drops down to zero and is replaced by the resistive crowbar.

In order to model the described case, the rotor resistance can be adapted to reflect the crowbar resistance and the firing of the crowbar is modelled by a rotor voltage step towards zero [17]. The action of the crowbar is out of the scope of this work, but all equations have been derived in a way that it will be very easy to perform that last step.

The equivalent diagram of the DFIG presented in [15] is recalled in Fig. 1.

B. Basis for the Analytical model

Table I presents the numerical values of the parameters of the considered machine. From the equivalent diagram of Fig. 1, it follows that

$$\underline{I}_\mu = \underline{I}_s + \underline{I}_r'. \tag{1}$$

Moreover, one can easily deduce the voltage equations, yielding

$$\underline{U}_s = R_s \underline{I}_s + \mathbf{j}(X_{\sigma,s} + X_h)\underline{I}_s + X_h \underline{I}_r' \tag{2}$$

$$\frac{\underline{U}_r'}{s} = \frac{R_r'}{s}\underline{I}_r' + \mathbf{j}(X_{\sigma,r}' + X_h)\underline{I}_r' + X_h \underline{I}_s, \tag{3}$$

TABLE I

Parameter values of the considered case machine of this paper

Description	Parameter	Value	
Apparent power	S_n	265.50	MVA
Rated voltage (rms)	U_n	18.00	kV
Rated current (rms)	I_n	8515.70	A
Nominal frequency (stator)	f_n	50.00	Hz
Mechanical speed	n_n	158.51	r/min
Number of poles	p	18.00	
Base impedance	Z_n	1.22	Ω
Stator resistance	R_s	4.5056	mΩ
	r_s	3.6920×10^{-3}	$p.u.$
Rotor resistance	R_r'	1.9364	mΩ
	r_r'	1.5867×10^{-3}	$p.u.$
Stator leakage reactance	$X_{\sigma,s}$	0.1525	Ω
	$x_{\sigma,s}$	1.9387	$p.u.$
Rotor leakage reactance	$X_{\sigma,r}'$	0.1957	Ω
	$x_{\sigma,r}'$	0.1604	$p.u.$
Magnetizing reactance	X_h	1.5886	Ω
	x_h	0.1249	$p.u.$

which have been published in [15]. They become in transient mode replacing the time derivative by their Laplace-form, written in pu

$$u_s = r_s i_s + \left(\frac{d}{dt} + \mathbf{j}\omega_s\right)\psi_s \tag{4}$$

$$u_r = r_r i_r + \left(\frac{d}{dt} + \mathbf{j}\Delta\omega\right)\psi_r \tag{5}$$

where the $'$-sign is omitted not to create confusion for the transient equation (x_s' and x_r') of the inductances. The slip is taken into account into the definition of $\Delta\omega = s\omega_\mathrm{s}$, as it is defined by

$$\Delta\omega = \omega_s - \omega_\text{mech} = \omega_s - \omega_s(1-s) = s\omega_s. \tag{6}$$

The fluxes (stator with subscript s and rotor with subscript r) are given by

$$\psi_s = x_s i_s + x_h i_r \tag{7}$$

$$\psi_r = x_h i_s + x_r i_r \tag{8}$$

with $x_s = x_{\sigma s} + x_{hs}$ and $x_r = x_{\sigma r} + x_{hr}$. The voltage equations are written in per unit (p.u.), in the stator reference frame aligned with the stator voltage phasor.

III. Fundamental DFIM transient equations

This section formulates the transient equations and relations for the different parts of the investigated large DFIM. Subsection III-A describes the importance of the initial conditions in terms of transient modelling. Then, Subsection III-B derives the stator and the rotor currents in terms of the stator and the rotor voltages in the Laplace domain. Subsection III-C introduces direct transient relations between the stator and rotor voltages and the fluxes in the DFIM. The steps to obtain the transient formulation of the rotor current is described in Subsection III-D. Further, the "large machine approximation" is introduced in Subsection III-E. Moreover, the validity of the simplification is explored. The transient torque harmonics prediction is then explored in Subsection III-F. Finally, an additional original contribution of this work is described in Subsection III-G on the modelling of the two-phase short-circuit.

A. Initial conditions

The principle of the derivation of the transient equations has been taken from [15] and is different from the ones presented in [14]. This contribution has also derived the complete set of equations as done in [14].

In predicting the DFIM the transients, some initial conditions (written with the subscript 'o') are needed. The stator voltage u_{s}, the speed n and the mechanical power p_{mec} are known. From these three parameters, one can deduce the initial values of the stator current ($i_{\mathrm{s}0}$), rotor ($i_{\mathrm{r}0}$) current and rotor voltage ($u_{\mathrm{r}0}$). For the stator and rotor fluxes (used to calculate the torque) their initial conditions are given by

$$u_s = r_s \cdot i_{\mathrm{s}0} + \mathbf{j}\omega_s\psi_{so} \tag{9}$$

$$\psi_{so} = \frac{u_s - r_s \cdot i_{so}}{\mathbf{j}\omega_s} \tag{10}$$

and

$$u_{ro} = r_r \cdot i_{ro} + \mathbf{j}\Delta\omega\psi_{ro} \tag{11}$$

$$\psi_{ro} = \frac{u_{ro} - r_r \cdot i_{ro}}{\mathbf{j}\Delta\omega}. \tag{12}$$

where eqs. (11) and (12) are written in the stator reference frame as stated in Section II.

B. Transient Equations for the Stator Current

The fundamental eqs. 4 and 5 can be made more compact by replacing their time-derivative d/dt by the Laplace-operator p.

$$u_s = r_s i_s + (p + \mathbf{j}\omega_s)\psi_s \tag{13}$$

$$u_r = r_r i_r + (p + \mathbf{j}\Delta\omega)\psi_r. \tag{14}$$

Then, the equation for the rotor flux, eq. (8), can be inserted into eq. (14) as follows

$$u_{\mathrm{r}} = [r_{\mathrm{r}} + (p + j\Delta\omega)x_{\mathrm{r}}]i_{\mathrm{r}} + (p + j\Delta\omega)x_{\mathrm{h}}i_{\mathrm{s}}, \tag{15}$$

$$i_{\mathrm{r}} = \frac{u_{\mathrm{r}} - (p + j\Delta\omega)x_{\mathrm{h}}i_{\mathrm{s}}}{r_{\mathrm{r}}[1 + (p + j\Delta\omega)T_{\mathrm{r}}]}, \tag{16}$$

where $T_r = x_r/r_r$. Eq. (16) for i_{r} can then be combined into eq. (13), yielding

$$\begin{aligned} u_{\mathrm{s}} =& \frac{p^2 + p[\frac{T_{\mathrm{s}}+T_{\mathrm{r}}}{T'_{\mathrm{s}}+T'_{\mathrm{r}}} + j(\omega_{\mathrm{s}} + \Delta\omega)]}{x_{\mathrm{r}}(1/T_{\mathrm{r}} + (p + j\Delta\omega))} i_{\mathrm{s}} \\ &+ \frac{\frac{1}{T_{\mathrm{s}}\cdot T'_{\mathrm{r}}}[1 + j\Delta\omega T_{\mathrm{r}} + j\omega_{\mathrm{s}}T_{\mathrm{s}}(1 + j\Delta\omega T'_{\mathrm{r}})]}{x_{\mathrm{r}}(1/T_{\mathrm{r}} + (p + j\Delta\omega))} i_{\mathrm{s}} \\ &+ \frac{x_{\mathrm{h}}}{x_{\mathrm{r}}}\frac{(p + j\omega_{\mathrm{s}})}{1/T_{\mathrm{r}} + (p + j\Delta\omega)} u_{\mathrm{r}}, \end{aligned} \tag{17}$$

$$\begin{aligned} \cong& \frac{(p + 1/T'_{\mathrm{s}} + j\omega_{\mathrm{s}})(p + 1/T'_{\mathrm{r}} + j\Delta\omega)}{x_{\mathrm{r}}(1/T_{\mathrm{r}} + (p + j\Delta\omega))} i_{\mathrm{s}} \\ &+ \frac{x_{\mathrm{h}}}{x_{\mathrm{r}}}\frac{(p + j\omega_{\mathrm{s}})}{1/T_{\mathrm{r}} + (p + j\Delta\omega)} u_{\mathrm{r}}, \end{aligned} \tag{18}$$

where $T_s = x_s/r_s$, $T'_{\mathrm{s}} = x'_s/r_s$ with $x'_s = x_{\sigma,\mathrm{s}} + x_{\mathrm{h}}x_{\sigma,\mathrm{r}}/x_r$ and $T'_{\mathrm{r}} = x'_r/r_s$ with $x'_r = x_{\sigma,\mathrm{r}} + x_{\mathrm{h}}x_{\sigma,\mathrm{s}}/x_s$. The numerator of eq. (17) is a second order polynom and its simplification using the "large machine approximation" is detailed in Section III-E. Eq. (17) is the exact equation of the stator current transfert function, while eq. (18) is the simplified one using the "large machine approximation".

Eq. (17) can be expressed in terms of the stator current, yielding

$$\begin{aligned} i_{\mathrm{s}} =& \frac{x_{\mathrm{r}}}{x_{\mathrm{s}}x'_{\mathrm{r}}}\frac{p + 1/T_{\mathrm{r}} + j\Delta\omega}{(p + 1/T'_{\mathrm{s}} + j\omega_{\mathrm{s}})(p + 1/T'_{\mathrm{r}} + j\Delta\omega)} u_{\mathrm{s}} \\ &+ \frac{x_{\mathrm{h}}}{x_{\mathrm{r}}}\frac{p + j\omega_{\mathrm{s}}}{(p + 1/T'_{\mathrm{s}} + j\omega_{\mathrm{s}})(p + 1/T'_{\mathrm{r}} + j\Delta\omega)} u_{\mathrm{r}}. \end{aligned} \tag{19}$$

The transient equation of the stator current can be found by applying an inverse Laplace-transform to the equation. In fact, it is not straightforward to find approximate equation for $i_{\mathrm{s}0}$, $i_{\mathrm{s}1}$ and $i_{\mathrm{s}2}$ (cf. Section III-F for the definition of these currents) as $\Delta\omega$ has a large amplitude variation and that the equations are not linear in terms of $\Delta\omega$ [17]. The prediction of the current calculation can be found using the exact solution to obtain the zeros of the numerator of eq. (17) as well as the coefficients $i_{\mathrm{s}0}$, $i_{\mathrm{s}1}$ and $i_{\mathrm{s}2}$.

C. Transient Equation for the Stator Flux

Rewriting the flux equations in matrix-form leads to

$$\begin{bmatrix} \psi_{\mathrm{s}} \\ \psi_{\mathrm{r}} \end{bmatrix} = \begin{pmatrix} x_{\mathrm{s}} & x_{\mathrm{h}} \\ x_{\mathrm{h}} & x_r \end{pmatrix} \begin{bmatrix} i_{\mathrm{s}} \\ i_{\mathrm{r}} \end{bmatrix}. \tag{20}$$

Inverting the matrix will provide equations of the currents in terms of the fluxes. After inverting them, one obtains

$$\begin{bmatrix} i_{\mathrm{s}} \\ i_{\mathrm{r}} \end{bmatrix} = \frac{1}{x_{\mathrm{s}}x_{\mathrm{r}} - x_{\mathrm{h}}^2} \begin{pmatrix} x_{\mathrm{r}} & -x_{\mathrm{h}} \\ -x_{\mathrm{h}} & x_{\mathrm{s}} \end{pmatrix} \begin{bmatrix} \psi_{\mathrm{s}} \\ \psi_{\mathrm{r}} \end{bmatrix}, \tag{21}$$

or

$$\begin{aligned} i_{\mathrm{s}} &= \frac{1}{x'_{\mathrm{s}}}\psi_{\mathrm{s}} - \frac{x_{\mathrm{h}}}{x'_{\mathrm{s}}x_{\mathrm{r}}}\psi_{\mathrm{r}} \\ i_{\mathrm{s}} &= \alpha\psi_{\mathrm{s}} + \beta\psi_{\mathrm{r}}, \end{aligned} \tag{22}$$

and for the rotor flux

$$\begin{aligned} i_{\mathrm{r}} &= -\frac{x_{\mathrm{h}}}{x'_{\mathrm{s}}x_{\mathrm{r}}}\psi_{\mathrm{s}} + \frac{1}{x'_{\mathrm{r}}}\psi_{\mathrm{r}} \\ i_{\mathrm{r}} &= \gamma\psi_{\mathrm{s}} + \delta\psi_{\mathrm{r}}, \end{aligned} \tag{23}$$

where

$$x'_{\mathrm{s}} = \frac{x_{\mathrm{s}}x_{\mathrm{r}} - x_{\mathrm{h}}^2}{x_{\mathrm{r}}}, \tag{24}$$

and

$$x'_{\mathrm{r}} = \frac{x_{\mathrm{s}}x_{\mathrm{r}} - x_{\mathrm{h}}^2}{x_{\mathrm{s}}}. \tag{25}$$

Note that $\beta = \gamma$, but it was more convenient to define two separate variables, i.e., to keep the "matrix thinking" in deriving the equations. Applying these expressions into the rotor voltage equation, eq. (14), leads to

$$\begin{aligned} u_{\mathrm{r}} &= r_{\mathrm{r}} i_{\mathrm{r}} + (p + j\Delta\omega)\psi_{\mathrm{r}} \\ &= r_{\mathrm{r}}\gamma\psi_{\mathrm{s}} + (r_{\mathrm{r}}\delta + (p + j\Delta\omega))\psi_{\mathrm{r}}. \end{aligned} \tag{26}$$

The solution in terms of ψ_{r} is

$$\psi_{\mathrm{r}} = \frac{u_{\mathrm{r}} - r_{\mathrm{r}}\gamma\psi_{\mathrm{s}}}{r_{\mathrm{r}}\delta + (p + j\Delta\omega)}. \tag{27}$$

This result can be incorporated into the stator voltage equation, eq. (13), yielding

$$\begin{aligned} u_{\mathrm{s}} &= r_{\mathrm{s}} i_{\mathrm{s}} + (p + j\omega_{\mathrm{s}})\psi_{\mathrm{s}} \\ &= \frac{((r_{\mathrm{s}}\alpha + (p + j\omega_{\mathrm{s}}))(r_{\mathrm{r}}\delta + (p + j\Delta\omega)) - r_{\mathrm{s}} r_{\mathrm{r}}\beta\gamma)\psi_{\mathrm{s}} + r_{\mathrm{s}}\beta u_{\mathrm{r}}}{r_{\mathrm{r}}\delta + (p + j\Delta\omega)}. \end{aligned} \tag{28}$$

This equation, eq. (27), in terms of ψ_{s} becomes

$$\begin{aligned} \psi_{\mathrm{s}} =& \frac{(r_{\mathrm{r}}\delta + (p + j\Delta\omega))u_{\mathrm{s}} - r_{\mathrm{s}}\beta u_{\mathrm{r}}}{(r_{\mathrm{s}}\alpha + (p + j\omega_{\mathrm{s}}))(r_{\mathrm{r}}\delta + (p + j\Delta\omega)) - r_{\mathrm{s}} r_{\mathrm{r}}\beta\gamma} \\ =& \frac{(r_{\mathrm{r}}\delta + (p + j\Delta\omega))}{(r_{\mathrm{s}}\alpha + (p + j\omega_{\mathrm{s}}))(r_{\mathrm{r}}\delta + (p + j\Delta\omega)) - r_{\mathrm{s}} r_{\mathrm{r}}\beta\gamma} u_{\mathrm{s}} \\ & - \frac{r_{\mathrm{s}}\beta}{(r_{\mathrm{s}}\alpha + (p + j\omega_{\mathrm{s}}))(r_{\mathrm{r}}\delta + (p + j\Delta\omega)) - r_{\mathrm{s}} r_{\mathrm{r}}\beta\gamma} u_{\mathrm{r}}. \end{aligned} \tag{29}$$

D. Transient Equation for the Rotor Current

The stator voltage equation, eq. (13), is solved to obtain i_{s}, which will be inserted into the rotor voltage equation, eq. (15), which will be solved to obtain the desired transfer function. Solving for the stator voltage equation leads to

$$i_{\mathrm{s}} = \frac{u_{\mathrm{s}} - (p + j\omega_{\mathrm{s}})x_{\mathrm{h}} i_{\mathrm{r}}}{r_{\mathrm{s}}(1 + (p + j\omega_{\mathrm{s}})T_{\mathrm{s}})}. \tag{30}$$

The result of eq. (30) can then be inserted into the rotor voltage equation, yielding

$$\begin{aligned} u_{\mathrm{r}} =& r_{\mathrm{r}}(1 + (p + j\Delta\omega)T_{\mathrm{r}})i_{\mathrm{r}} + (p + j\Delta\omega)x_{\mathrm{h}} i_{\mathrm{s}} \\ =& \frac{r_{\mathrm{r}} r_{\mathrm{s}}(1 + (p + j\Delta\omega)T_{\mathrm{r}})(1 + (p + j\omega_{\mathrm{s}})T_{\mathrm{s}})}{r_{\mathrm{s}}(1 + (p + j\omega_{\mathrm{s}})T_{\mathrm{s}})} i_{\mathrm{r}} \\ & - \frac{(p + j\Delta\omega)(p + j\omega_{\mathrm{s}})x_{\mathrm{h}}^2}{r_{\mathrm{s}}(1 + (p + j\omega_{\mathrm{s}})T_{\mathrm{s}})} i_{\mathrm{r}} \\ & + \frac{(p + j\Delta\omega)x_{\mathrm{h}}}{r_{\mathrm{s}}(1 + (p + j\omega_{\mathrm{s}})T_{\mathrm{s}})} u_{\mathrm{s}}. \end{aligned} \tag{31}$$

Solving eq. (31) in terms of i_{r} leads to the needed expression.

E. Simplification of the Poles of the Transfer Function - the Large Machine Approximation

Recalling the numerator of eq. (17) leads to

$$\begin{aligned} & p^2 + p[\frac{T_{\mathrm{s}} + T_{\mathrm{r}}}{T_{\mathrm{s}}' + T_{\mathrm{r}}'} + j(\omega_{\mathrm{s}} + \Delta\omega)] \\ & + \frac{1}{T_{\mathrm{s}} \cdot T_{\mathrm{r}}'}[1 + j\Delta\omega T_{\mathrm{r}} + j\omega_{\mathrm{s}} T_{\mathrm{s}}(1 + j\Delta\omega T_{\mathrm{r}}')] = 0. \end{aligned} \tag{32}$$

In the field of large electrical machines, the following inequalities can be considered as fulfilled (refer to [15])

$$T_{\mathrm{r}} > T_{\mathrm{s}} >> T_{\mathrm{r}}' >> T_{\mathrm{s}}' >> 1/\omega_{\mathrm{s}} \tag{33}$$

or

$$\omega_{\mathrm{s}} >> 1/T_{\mathrm{s}}' > 1/T_{\mathrm{r}}' >> 1/T_{\mathrm{s}} > 1/T_{\mathrm{r}}. \tag{34}$$

The inequalities are also called the "large machine approximation". On purpose, $\Delta\omega$ was deliberately not used in the inequalities as it can change in the range $-0.1\omega_{\mathrm{s}}$ to $0.1\omega_{\mathrm{s}}$. This will help us to simplify the equation of the poles and demonstrate that the poles (p_1 and p_2) can be expressed by

$$p_1 = -1/T_{\mathrm{s}}' - j\omega_{\mathrm{s}}, \tag{35}$$

$$p_2 = -1/T_{\mathrm{r}}' - j\Delta\omega, \tag{36}$$

at leading order. Eq. (32) is quadratic in p, so that the exact equation can be found for its solutions which will expressed using the following notation

$$p_{1/2} = -\frac{1}{2}\zeta \pm \frac{1}{2}\sqrt{\eta - \nu} \tag{37}$$

defining the following constants

$$\zeta = [\frac{T_{\mathrm{s}} + T_{\mathrm{r}}}{T_{\mathrm{s}} \cdot T_{\mathrm{r}}'} + j(\omega_{\mathrm{s}} + \Delta\omega)] \tag{38}$$

$$\eta = (\frac{T_{\mathrm{s}} + T_{\mathrm{r}}}{T_{\mathrm{s}} \cdot T_{\mathrm{r}}'} + j(\omega_{\mathrm{s}} + \Delta\omega))^2 \tag{39}$$

$$\nu = \frac{4}{T_{\mathrm{s}} T_{\mathrm{r}}'}(1 + j\Delta\omega T_{\mathrm{r}} + j\omega_{\mathrm{s}} T_{\mathrm{s}}(1 + j\Delta\omega T_{\mathrm{r}}'))^2. \tag{40}$$

Let's first expand the term η and simplify it applying the inequalities

$$\begin{aligned} \eta =& \frac{T_{\mathrm{s}} + T_{\mathrm{r}}}{T_{\mathrm{s}} \cdot T_{\mathrm{r}}'}^2 - (\Delta\omega + \omega_{\mathrm{s}})^2 + 2j(\Delta\omega + \omega_{\mathrm{s}})\frac{T_{\mathrm{s}} + T_{\mathrm{r}}}{T_{\mathrm{s}} \cdot T_{\mathrm{r}}'} \\ =& -\omega_{\mathrm{s}}^2[1 + 2\frac{\Delta\omega}{\omega_{\mathrm{s}}} + \frac{\Delta\omega^2}{\omega_{\mathrm{s}}^2} - \frac{1}{\omega_{\mathrm{s}}^2}(\frac{T_{\mathrm{s}} + T_{\mathrm{r}}}{T_{\mathrm{s}} \cdot T_{\mathrm{r}}'})^2 \\ & - 2j\frac{T_{\mathrm{s}} + T_{\mathrm{r}}}{T_{\mathrm{s}} \cdot T_{\mathrm{r}}'}(\frac{\Delta\omega}{\omega_{\mathrm{s}}^2} + \frac{1}{\omega_{\mathrm{s}}})]. \end{aligned} \tag{41}$$

As η is in the square root it is very interesting to simplify the equation by taking $-\omega_{\mathrm{s}}^2$ in evidence. The minus sign was used in order to get j after applying the square root. Neglecting the terms in $1/\omega_{\mathrm{s}}^2$ leads to

$$\begin{aligned} \eta \cong& -\omega_{\mathrm{s}}^2[1 + 2\frac{\Delta\omega}{\omega_{\mathrm{s}}} + \frac{1}{\omega_{\mathrm{s}}} \cdot (-2j\frac{T_{\mathrm{s}} + T_{\mathrm{r}}}{T_{\mathrm{s}} \cdot T_{\mathrm{r}}'})] \\ \cong& -\omega_{\mathrm{s}}^2(1 + \alpha\frac{\Delta\omega}{\omega_{\mathrm{s}}} + \beta\frac{1}{\omega_{\mathrm{s}}}). \end{aligned} \tag{42}$$

Continuing with the simplification of ν

$$\begin{aligned} \nu =& -\frac{4}{T_{\mathrm{s}} \cdot T_{\mathrm{r}}'}(1 + j\Delta\omega T_{\mathrm{r}} + j\omega_{\mathrm{s}} T_{\mathrm{s}} + j\omega_{\mathrm{s}} T_{\mathrm{s}} j\Delta\omega T_{\mathrm{r}}') \\ =& -\omega_{\mathrm{s}}^2(\frac{4}{\omega_{\mathrm{s}}^2 T_{\mathrm{s}} T_{\mathrm{r}}'} + j\frac{\Delta\omega}{\omega_{\mathrm{s}}^2} T_{\mathrm{s}}\frac{4}{T_{\mathrm{s}} \cdot T_{\mathrm{r}}'} + j\frac{4}{\omega_{\mathrm{s}} \cdot T_{\mathrm{r}}'} + 4j^2\frac{\Delta\omega}{\omega_{\mathrm{s}}}). \end{aligned} \tag{43}$$

Neglecting once again the terms in $1/\omega_s^2$ leads to

$$\nu \cong -\omega_s^2(-4\frac{\Delta\omega}{\omega_s} + j\frac{4}{\omega_s \cdot T_r'}). \tag{44}$$

Calculating the term in the square root, i.e., making $\eta - \nu$ leads to

$$\eta - \nu = -\omega_s^2(1 + 2\frac{\Delta\omega}{\omega_s} + \beta'\frac{1}{\omega_s}) \tag{45}$$

where β' is given by

$$\beta' = -2j\frac{T_s + T_r}{T_s \cdot T_r'} + \frac{4j}{T_r'}. \tag{46}$$

The equation under the square root becomes then

$$\begin{aligned}\sqrt{-\omega_s^2(1 + 2\frac{\Delta\omega}{\omega_s} + \beta'\frac{1}{\omega_s})} &\cong j\omega_s(1 - \frac{\Delta\omega}{\omega_s} + \frac{\beta'}{2}\frac{1}{\omega_s}) \\ &= j(\omega_s - \Delta\omega) + j\frac{\beta'}{2} \\ &= j(\omega_s - \Delta\omega) + \frac{T_s + T_r}{T_s \cdot T_r'} - \frac{2}{T_r'}. \end{aligned} \tag{47}$$

The first solution of the equation p_1 becomes then

$$\begin{aligned} p_1 &= -\frac{1}{2}\frac{T_s + T_r}{T_s \cdot T_r'} - \frac{j}{2}(\Delta\omega + \omega_s) - \frac{1}{2}j(\omega_s - \Delta\omega) \\ &\quad -\frac{1}{2}\frac{T_s + T_r}{T_s \cdot T_r'} + \frac{1}{T_r'} \\ &= -\frac{T_s + T_r}{T_s \cdot T_r'} + \frac{1}{T_r'} - j\omega_s = -\frac{1}{T_r'}(\frac{T_s + T_r}{T_s} - 1) - j\omega_s \\ &= -\frac{T_r}{T_s \cdot T_r'} - j\omega_s = -\frac{1}{T_s'} - j\omega_s. \end{aligned} \tag{48}$$

For the second solution p_2 one obtains

$$\begin{aligned} p_2 &= -\frac{1}{2}\frac{T_s + T_r}{T_s \cdot T_r'} - \frac{1}{2}j(\Delta\omega + \omega_s) + \frac{1}{2}j(\omega_s - \Delta\omega) \\ &\quad +\frac{1}{2}\frac{T_s + T_r}{T_s \cdot T_r'} - \frac{1}{T_r'} \\ &= -\frac{1}{T_r'} - j\Delta\omega. \end{aligned} \tag{49}$$

Fig. 2 shows the evolution if the real part and imaginary part of p_1 and p_2 for different values of $\Delta\omega$. One can see that at leading order, the poles behave like the simplified equations predicts.

F. Torque Harmonics for a Three-Phase Short-Circuit, or Three-Phase Faulty Synchronization

To exclude any excitation of a mechanical eigenmode of in the stator or rotor of the generator, one needs to determine the frequency of the torque harmonics. From eq. (30) one can deduce that the stator current is given by

$$\begin{aligned} i_s &= i_{s0} + i_{s1}\exp(-t/T_s')\sin(\omega_s t) \\ &\quad + i_{s2}\exp(-t/T_r')\sin(\Delta\omega t) \end{aligned} \tag{50}$$

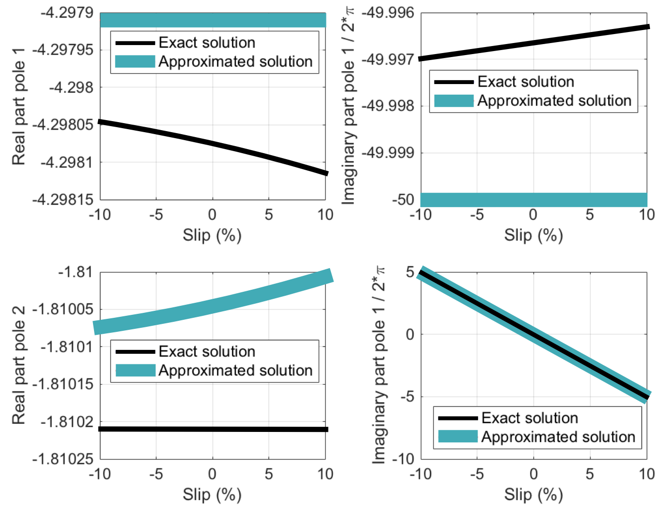

Fig. 2. Evolution of the poles p_1 and p_2 in function of $\Delta\omega$

where i_{s0}, i_{s1} and i_{s2} are obtained from the corresponding transfer function. Similarly, the stator flux is obtained by the stator current, starting from eq. (29) and is given by

$$\begin{aligned} \psi_s &= \psi_{s0} + \psi_{s1}\exp(-t/T_s')\sin(\omega_s t) \\ &\quad + \psi_{s2}\exp(-t/T_r')\sin(\Delta\omega t) \end{aligned} \tag{51}$$

where ψ_{s0}, ψ_{s1}, ψ_{s2} are obtained from the corresponding transfer function. The torque is given by

$$t_{em} = \frac{3}{2} \cdot p \cdot \mathbb{Im}\{\psi_s^* \cdot i_s\}. \tag{52}$$

The interesting part on the torque harmonics is to check if there could be any resonance between the mechanical system and the foundation, i.e., it is not mandatory to calculate each component but just its frequency dependence so that

$$\begin{aligned} t_{em} &\sim \sin(\omega_s t)^2 + \sin(\omega_s t) + \sin(\Delta\omega t)\sin(\omega_s t) + \sin(\Delta\omega t)^2 \\ &\sim \cos(0 \cdot t) + \sin(\omega_s t) + \cos(2\omega_s t) + \cos((\omega_s \pm \Delta\omega)t) \\ &\quad + \cos(2\Delta\omega t), \end{aligned} \tag{53}$$

where the sign $\sim$ means "is linearly proportional to". The torque presents, therefore, the following frequencies during a three-phase short-circuit or a three-phase faulty synchronisation

$$f_1 = 2\Delta\omega \tag{54}$$

$$f_2 = \omega_s \pm \Delta\omega \tag{55}$$

$$f_3 = \omega_s \tag{56}$$

$$f_4 = 2\omega_s. \tag{57}$$

G. Modelling the Two-Phase Short-Circuit

Until now, there were no exact analytical equations for the current or torque of a two-phase short-circuit in the dq-rotating frame. Based on previous works on the DC-Decay tests (two-phase short-circuit) in a synchronous machine [18], which could be calculated exactly analytically, it has been decided to search for an analytical equation for the voltage step in the dq-frame, which is the only reference frame that would lead to analytical equations for a rotating machine [18], [19]. The two-phase short-circuit is characterised by the following equation

$$u_a = u_b. \tag{58}$$

This equation means nothing else than, the fact that the two voltages will be the same after the short-circuit. Supposing, in addition, that the machine is star connected, leads to the following equation

$$\begin{aligned} u_\mathrm{a} + u_\mathrm{b} + u_\mathrm{c} &= 0 \\ 2u_\mathrm{a} + u_\mathrm{c} &= 0. \end{aligned} \tag{59}$$

In order to obtain the voltages after the short-circuit, the reaction of the voltage on phase c must be known or supposed known after the short-circuit. Before the short-circuit the voltage on this phase is given neither by the machine (through the induced voltage) or by the grid. Just after the short-circuit (a few milliseconds after), the currents in the machine will not have any discontinuity (as the current, as well as the fluxes, are state variables), so that the voltage in phase c will remain the same. The grid voltage, as phase c, is not affected by the short-circuit will also not change. As there is no change in the voltage of phase c at the beginning of the short-circuit, then there will be no other changes in this voltage during the whole short-circuit. Mathematically speaking, the phase voltage equation could be expressed as

$$u_i = r_i i_i + \sum_j \frac{d\psi_{ij}}{dt}. \tag{60}$$

To change the voltage u_i one should change instantaneously the flux ψ_{ik} which is not possible as it is a continuous state-variable. The current will not change instantaneously as the current is a linear combination of fluxes. As a result,

$$u_\mathrm{c} = u_\mathrm{s}, \tag{61}$$

where u_s is the stator voltage phasor before the short-circuit. In this case, it is interesting to keep Park's reference frame aligned with the stator voltage in order to get a real number. Knowing this, the stator voltage in the abc-frame is known before and after the short-circuit, where its given by

$$u_\mathrm{a} = -u_\mathrm{c}/2 \tag{62}$$

$$u_\mathrm{b} = -u_\mathrm{c}/2 \tag{63}$$

$$u_\mathrm{c} = u_\mathrm{c}. \tag{64}$$

In order to obtain the voltage in the dq-frame, it is sufficient to take Park's transformation of this voltage. After some trivial trigonometric operations, one obtains the voltage in the rotating frame, yielding

$$u_d = -\frac{u}{2}\sin(2\omega_\mathrm{s}t) \tag{65}$$

$$u_q = -\frac{u}{2}(1+\cos(2\omega_\mathrm{s}t)), \tag{66}$$

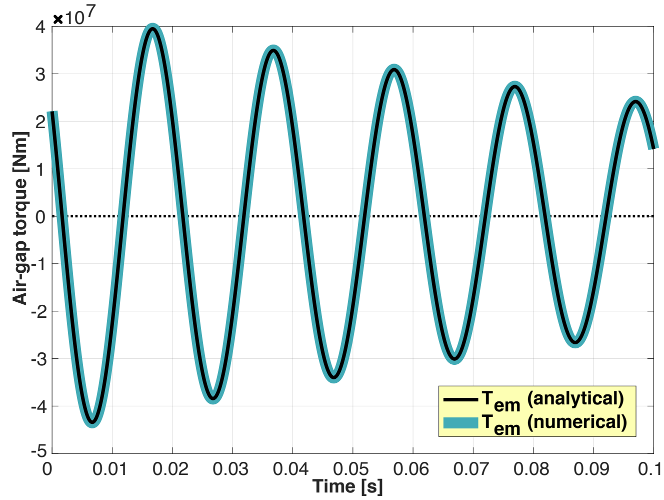

Fig. 3. Air-gap torque (ASM) three-phases short-circuit.

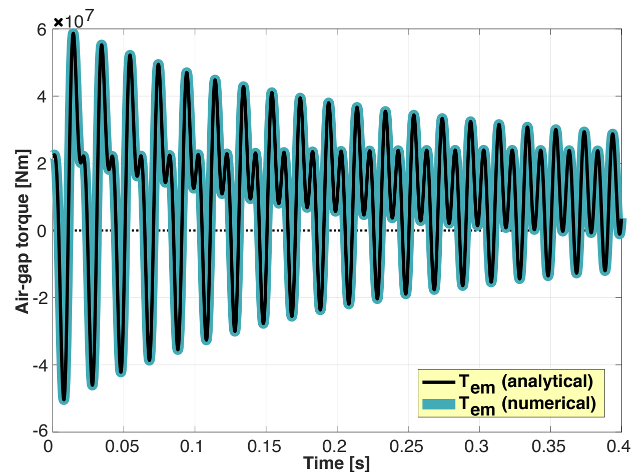

Fig. 4. Air-gap torque (ASM) two-phases short-circuit. The torque is constant before the short-circuit as per modelling hypothesis.

which is an original contribution of this work. With these voltages, it is straightforward to obtain the Laplace-transformation of them to calculate the short-circuit currents.

To know the torque harmonics appearing during a 2-phase short-circuit or faulty synchronisation, one only needs to apply the technique described in section III-F using the voltage equations (65) and (66).

IV. Validation of the Analytical Equations

This section presents the validation of the analytical equations developed in Section III. The validation is done in the SIMSEN software environment using the parameters defined in Table I (handpicked case study). The software assumes an equivalent diagram as per figure 1 and applies the same hypothesis as the one defined in section II-A. The analytical equations are compared to numerical solutions. Practically speaking, one enters the same parameters (refer to Table I) and initial conditions and compares the output. The limitations of the validation depend on the modelling hypothesis II-A.

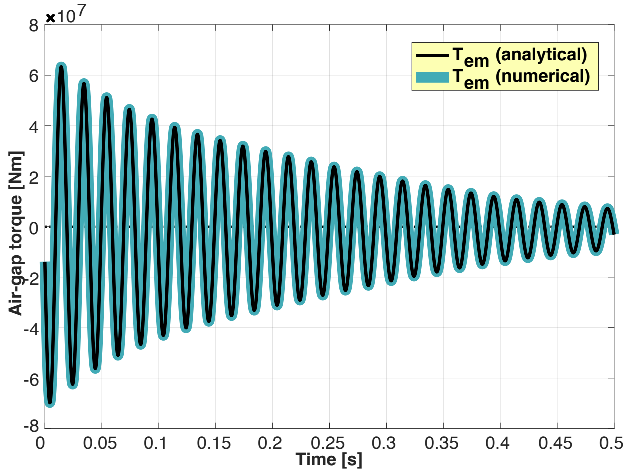

Fig. 5. Air-gap torque (DFIM) three-phases short-circuit. The torque is constant before the short-circuit as per modelling hypothesis.

The equivalent diagram parameters for the ASM (asynchronous machine) and the DFIG (doubly-fed induction generator) were the same. The ASM is, therefore, a virtual machine, while the DFIG can be considered as the real case. The ASM case was only used to simplify the model to be validated in the case of a two-phase short-circuit. The DFIG is operating at rated operation (over-excited) before the short-circuit, while the ASM is operating at the same equivalent operating point (same active power) before the short-circuit for both the two-phase and three-phase short-circuit. As the validation for the two-phase short-circuit only depends on the stator voltage equation, it has been decided to perform it only on the ASM, i.e., the simplest case. Whereas given the premise that this case is correct, then the validation for the DFIG case is implicit. For the DFIG, it has been decided to validate the three-phase short-circuit only to validate both cases implicitly. Figs. 3, 4 and 5 present the air-gap curves for the ASM machine in three-phase and two-phase short-circuit and DFIG in the case of a three-phase short-circuit. All curves agrees well with the simulated curves in SIMSEN.

V. Conclusion

This paper proposes to simplify and improve the transient analysis of double-fed induction machines (DFIMs) by a detailed analytical model. The idea provides a precise frequency indication of the torque harmonics and a quantitative value for the torque amplitude. Moreover, the "large machine approximation" is introduced to the analytical model, and it is shown to be valid in the presented case study. Finally, the transient behaviour of the DFIM under two-phase and three-phase short-circuit scenarios show excellent agreement with simulations. Analytically, the amplitude and the time constants of the transient are governed by the parameter values, which are sensitive to the modelling assumption taken (FE-simulation, experiment, etc.). Nevertheless, the main goal of the proposed approach is to provide a "go/no-go" decision based on a frequency-based determination, where those effects are marginal. In order to improve further, more detailed parameter values, as well as complete power electronics and control actions can be taken into account, if needed.

References

[1] M. Debouza and A. Al-Durra, "Grid ancillary services from doubly fed induction generator-based wind energy conversion system: A review," *IEEE Access*, vol. 7, pp. 7067–7081, 2019.

[2] Yong Liao, Li Ran, G. A. Putrus, and K. S. Smith, "Evaluation of the effects of rotor harmonics in a dfig with harmonic induced speed ripple," *IEEE Trans. Energy Convers.*, vol. 18, no. 4, pp. 508–515, 2003.

[3] S. Djurovic, D. S. Vilchis-Rodriguez, and A. C. Smith, "Supply induced interharmonic effects in wound rotor and dfigs," *IEEE Trans. Energy Convers.*, vol. 30, no. 4, pp. 1397–1408, 2015.

[4] G. Mv and N. P. Padhy, "PHIL experimentation on fault ride through behavior of doubly fed induction generator based wind system in the presence of fault current limiter," *IEEE Trans. Ind. Appl.*, pp. 1–1, 2020.

[5] N. Jabbour, E. Tsioumas, C. Mademlis, and E. Solomin, "A highly effective fault-ride-through strategy for a wind energy conversion system with DFIG," *IEEE Trans. Power Electron.*, pp. 1–1, 2020.

[6] H. Nian and Y. Jiao, "Improved virtual synchronous generator control of DFIG to ride-through symmetrical voltage fault," *IEEE Trans. Energy Convers.*, pp. 1–1, 2019.

[7] G. Pannell, D. J. Atkinson, and B. Zahawi, "Analytical study of grid-fault response of wind turbine doubly fed induction generator," *IEEE Trans. Energy Convers.*, vol. 25, no. 4, pp. 1081–1091, Dec 2010.

[8] Y. Deng, Z. Xing, and Q. Zhang, "Analysis of electromagnetic transient characteristics of DFIG under grid voltage swell," *CPSS Trans. Power Electron. Appl.*, vol. 3, no. 2, pp. 111–118, June 2018.

[9] S. Tohidi, "Analysis and simplified modelling of brushless DFIM in synchronous mode of operation," *IET Elect. Power Appl.*, vol. 10, no. 2, pp. 110–116, 2016.

[10] M. Yousefian, H. A. Zarchi, and H. Gorginpour, "Modified steady-state modelling of brushless DFIG taking core loss components into account," *IET Elect. Power Appl.*, vol. 13, no. 9, pp. 1402–1412, 2019.

[11] Z. M. Salameh and L. F. Kazda, "Analysis of the double output induction generator using direct three-phase model part ii - harmonic analysis," *IEEE Trans. Energy Convers.*, vol. EC-2, no. 2, pp. 182–188, 1987.

[12] M. Zhou, Z. Dong, H. Li, C. Gan, G. Li, and Y. Liu, "Coordinated control of dfig based wind farms and sgs for improving transient stability," *IEEE Access*, vol. 6, pp. 46 844–46 855, 2018.

[13] D. Kim, Y. Moon, and H. Nam, "A new simplified doubly fed induction generator model for transient stability studies," *IEEE Trans. Energy Convers.*, vol. 30, no. 3, pp. 1030–1042, Sep. 2015.

[14] K. W. Kanelis, "Analytical equations of the induction machine," in *Proc. Int. Conf. Elect. Mach. (ICEM)*, Sep. 2016, pp. 2854–2860.

[15] J. Chatelain, "Machines électriques, volume x," *Traité dâ€™électricité series, Presses Polytechniques. PPUR, Lausanne, ppur Édition*, 2013.

[16] I. Canay, "Extended synchronous-machine model for the calculation of transient processes and stability," *Electric machines and Electromechanics*, vol. 1, no. 2, pp. 137–150, 1977.

[17] F. M. Maurer, "Electrical effects in winding of large electrical AC machines application to advanced large size DFIM," EPFL, Tech. Rep., 2019.

[18] F. Maurer, "Détermination des paramétres de la machine synchrone par essais "DC-Decay"," *Master thesis, EPFL*, 2009.

[19] F. Maurer, M. T. Xuan, and J. Simond, "Two full parameter identification methods for synchronous machine applying DC-decay tests for a rotor in arbitrary position," *IEEE Trans. Ind. Appl.*, vol. 53, no. 4, pp. 3505–3518, July 2017.

Frederic Maurer received the M.Sc. in 2009 and the Ph.D. degree in 2019 from the Swiss Federal Institute of Technology in Lausanne (EPFL), respectively. Since april 2009, he is working for Alstom Hydro (now GE Hydro) in different position: R&D engineer in the generator technology center, Lead electrical engineer and technical project manager.

Jonas Kristiansen Nøland (S'14-M'17) received the Ph.D. degree in eng. physics from Uppsala University, Uppsala, Sweden, in 2017. He is currently an Associate Professor with the Norwegian University of Science and Technology (NTNU), Trondheim, Norway. Dr. Nøland is serving as an Editor for the IEEE TRANSACTIONS ON ENERGY CONVERSION.